



HAL
open science

Influence of fumarate on interspecies electron transfer and the metabolic shift induced in *Clostridium pasteurianum* by *Geobacter sulfurreducens*

María Fernanda Pérez-Bernal, Roland Berthomieu, Elie Desmond-Le Quéméner, Nicolas Bernet, Eric Trably

► To cite this version:

María Fernanda Pérez-Bernal, Roland Berthomieu, Elie Desmond-Le Quéméner, Nicolas Bernet, Eric Trably. Influence of fumarate on interspecies electron transfer and the metabolic shift induced in *Clostridium pasteurianum* by *Geobacter sulfurreducens*. *Journal of Applied Microbiology*, 2024, 135 (5), pp.lxae122. 10.1093/jambio/lxae122 . hal-04614157

HAL Id: hal-04614157

<https://hal.inrae.fr/hal-04614157v1>

Submitted on 5 Aug 2024

HAL is a multi-disciplinary open access archive for the deposit and dissemination of scientific research documents, whether they are published or not. The documents may come from teaching and research institutions in France or abroad, or from public or private research centers.

L'archive ouverte pluridisciplinaire **HAL**, est destinée au dépôt et à la diffusion de documents scientifiques de niveau recherche, publiés ou non, émanant des établissements d'enseignement et de recherche français ou étrangers, des laboratoires publics ou privés.

Influence of fumarate on interspecies electron transfer and the metabolic shift induced in *Clostridium pasteurianum* by *Geobacter sulfurreducens*

María Fernanda Pérez-Bernal^{1*}, Roland Berthomieu¹, Elie Desmond- Le Quéméner¹, Nicolas Bernet¹, Eric Trably¹

¹INRAE, Univ Montpellier, LBE, 102 avenue des Etangs, 11100, Narbonne, France

***Corresponding author full address:**

Dr. María Fernanda Pérez-Bernal

maria-fernanda.perez-bernal@inrae.fr

INRAE - LBE UR050

Laboratoire De Biotechnologie De L'Environnement

102 Avenue des Étangs, 11100 Narbonne · France

Tel: +33 468 425 151

Running head: Influence of soluble TEA during IET

ABSTRACT

Aims: In previous studies, it was demonstrated that co-culturing *Clostridium pasteurianum* and *Geobacter sulfurreducens* triggers a metabolic shift in the former during glycerol fermentation. This shift, attributed to interspecies electron transfer and the exchange of other molecules, enhances the production of 1,3-propanediol at the expense of the butanol pathway. The aim of this investigation is to examine the impact of fumarate, a soluble compound usually used as an electron acceptor for *G. sulfurreducens*, in the metabolic shift previously described in *C. pasteurianum*.

Methods and results: Experiments were conducted by adding along with glycerol, acetate and different quantities of fumarate in co-cultures of *G. sulfurreducens* and *C. pasteurianum*. A metabolic shift was exhibited in all the co-culture conditions. This shift was more pronounced at higher fumarate concentrations. Additionally, we observed *G. sulfurreducens* growing even in the absence of fumarate and utilizing small amounts of this compound as an electron donor rather than an electron acceptor in the co-cultures with high fumarate addition.

Conclusions: This study provided evidence that interspecies electron transfer continues to occur in the presence of a soluble electron acceptor, and the metabolic shift can be enhanced by promoting the growth of *G. sulfurreducens*.

Impact statement: Our findings offer a novel approach for optimizing propanediol production from glycerol, opening possibilities for extending research to other electroactive-fermentative couples as tools for the obtaining higher value-added compounds.

Keywords: Interspecies electron transfer, fermentation, electro-fermentation, co-culture, microbial interaction, metabolic shift

INTRODUCTION

Cell metabolism allows living organisms to obtain energy for growth, maintenance, and survival through respiration, photosynthesis, or fermentation. For this purpose, microbial cells must constantly incorporate nutrients and then undergo a series of transformations, which are redox reactions based on electron transfer. Most living organisms conduct these redox reactions inside the cells by incorporating soluble or gaseous compounds (Kato 2015). Nevertheless, some microorganisms have the astounding ability to exchange electrons with solid external electron donors or acceptors in a process known as extracellular electron transfer (EET), also considered a type of microbial respiration (Kato 2015; Kracke et al. 2018). The ability of these microorganisms usually called electroactive bacteria (EABs) to transport electrons beyond their cell wall has been known for more than a century (Potter 1911).

Over the past decade, EET processes have gained attention mainly in the fields of microbial ecology, microbial physiology, and biotechnology (Kato 2015). The latter is reflected by the development of microbial electrochemical technologies (METs) in which redox reactions on electrodes are catalyzed by microbes for the production of electricity, the treatment of wastewater and/or the production of valuable products (Kracke, Vassilev and Krömer 2015). Recently, the development of electro-fermentation (EF), a process in which the electrode is used to modulate a spontaneous fermentation (Moscoviz et al. 2016), resulted in interesting effects. In EF, the electrode provides a supplementary electron source or sink to slightly modify the microbial intracellular redox balance, this can in turn deeply modify microbial gene expression and metabolism (Kato 2015). EF aims to increase the release of specific compounds and minimize the formation of undesirable by-products (Choi and Sang 2016; Kracke et al. 2018). In particular, EF does not require high current densities to significantly increase the targeted compounds as in other METs (Moscoviz et al. 2016).

Investigation of EET has recently been extended to interspecies extracellular electron transfer (IET), a type of relation that allows the cooperation between microorganisms in environments with limited nutrient conditions (Benomar et al. 2015). The ability of some

microorganisms to perform IET offers an efficient and cost-effective alternative to the electrode-bacteria EF approach to steer metabolic pathways (Moscoviz et al. 2017b).

During classic glycerol fermentation by *Clostridium pasteurianum*, butanol synthesis is the energetically preferred pathway (Moon et al. 2011; Krasňan et al. 2018) with 1,3-propanediol (1,3-PDO), ethanol, butyrate, acetate, lactate, CO₂ and H₂ as co-products. 1,3-PDO as the main co-product, is essential for balancing the intracellular reducing power through NAD⁺ regeneration (Krasňan et al. 2018). The possibility to change the metabolic products from glycerol fermentation of *C. pasteurianum* through EF, with electrons provided by an EAB, *Geobacter sulfurreducens*, instead of a cathode, was first investigated by Moscoviz et al., (2017b). *G. sulfurreducens* can utilize various electron acceptors, including Fe(III)-citrate, Co(III), U(VI), S⁰, fumarate, and malate, while oxidizing acetate (Lovley et al. 2011). In this study, together with the fermentable substrate for *C. pasteurianum*, acetate was added as a carbon source and electron donor for *G. sulfurreducens*, but without a terminal electron acceptor (TEA). The IET between these two species was successfully demonstrated. While *C. pasteurianum* underwent a shift in metabolite's distribution towards a higher 1,3-PDO production (+37 %), an increase in the number of cells of *G. sulfurreducens* was observed. This indicated the use of *C. pasteurianum* as final electron acceptor by *G. sulfurreducens* while oxidizing acetate. Recently, Berthomieu et al. (2022) performed a differential gene expression analysis to explain the mechanisms behind the interactions among these species. Their findings allowed them to propose a putative model in which IET is not the sole factor responsible for the observed metabolic shift. Indeed, proteins related to electron transfer, such as a transmembrane FMN-binding polyferredoxin and a cytochrome b5-rubredoxin, were overexpressed. More importantly, a downregulation of the cobalamin synthesis of *C. pasteurianum* during the co-culture with *G. sulfurreducens* was observed. Cobalamin is a cofactor for 1,3-PDO production; thus, it was hypothesized that the interaction between these strains and the consequent metabolic shift was mainly due to a mediated interaction through a molecule expelled in the medium by *G. sulfurreducens*, such as a cobamide.

The aim of this study was to investigate the influence of fumarate in the interactions between *C. pasteurianum* and *G. sulfurreducens* in co-cultures with, respectively, glycerol as fermentable substrate, and acetate as carbon source and electron donor. The addition of increasing concentrations of fumarate, largely used as a soluble electron acceptor to grow *G. sulfurreducens*, was studied to evaluate the effect on IET and in the metabolism of both strains when the interaction is not forced or essential for either them.

MATERIALS AND METHODS

Bacterial strains

G. sulfurreducens DSM 12127 and *C. pasteurianum* DSM 525 were purchased from the German Collection of Microorganisms and Cell Cultures GmbH (DSMZ) (Braunschweig, Germany). Hungate-type techniques (Hungate 1969) modified by (Miller and Wolin 1974) were used to cultivate both strains. *G. sulfurreducens* and *C. pasteurianum* were routinely cultivated according to specifications of the DSMZ in media 826 and 54b respectively. The medium 826 contained (per liter of distilled water): 1.50 g NH₄Cl, 0.60 g Na₂HPO₄, 0.10 g KCl, 0.82 g Na-acetate, 8.00 Na₂-fumarate, 10 mL modified Wolin's mineral solution, and 10 mL Wolin's vitamin solution. The modified Wolin's mineral solution contained (per liter of distilled water): 1.50 g nitriloacetic acid, 3.00 g MgSO₄·7H₂O, 0.50 g MnSO₄·H₂O, 1.00 g NaCl, 0.10 g FeSO₄·7H₂O, 0.18 g CoSO₄·7H₂O, 0.10 g CaCl₂·2H₂O, 0.18 g ZnSO₄·7H₂O, 0.01 g CuSO₄·5H₂O, 0.02 g AlK(SO₄)₂·12H₂O, 0.01 g H₃BO₃, 0.01 g Na₂MoO₄·2H₂O, 0.03 g NiCl₂·6H₂O, 0.30 mg Na₂SeO₃·5H₂O, and 0.40 mg Na₂WO₄·2H₂O. The Wolin's vitamin solution was composed (per liter of distilled water) of: 2 mg biotin, 2 mg folic acid, 10 mg pyridoxine hydrochloride, 5 mg thiamine HCl, 5 mg riboflavin, 5 mg nicotinic acid, 5 mg Ca D-(+)-pantothenate, 0.1 mg cobalamin, 5 mg p-aminobenzoic acid, and 5 mg (DL)-alpha-lipoic acid. The medium 54b contained (per liter of distilled water): 20.00 g glucose, 10.00 g yeast extract, and 20.00 g CaCO₃.

Media and growth conditions

The mineral medium (M1) used for pre-culture of both strains and fermentation batch tests was composed (per liter of distilled water) of: 2.00 g NH₄Cl, 0.75 g KCl, 2.45 g NaH₂PO₄, 4.58 g Na₂HPO₄, 0.28 g Na₂SO₄, 0.26 g MgCl₂·6H₂O, 2.9 mg CaCl₂·H₂O, 0.50 g L-cysteine as reductant, 1 mL resazurin solution 0.1% (w/v), 0.1 g yeast extract and, 10 mL of Modified Wolin's mineral solution. The medium was boiled, flushed with N₂, and dispensed into 120 mL serological bottles with a working volume of 50 mL under the same N₂ gas atmosphere to ensure anaerobic conditions. Subsequently, the bottles were sealed with butyl rubber stoppers and aluminum crimp seals, followed by sterilization through autoclaving at 121 °C for 15 minutes. After sterilization and prior to inoculation, the following compounds were added from sterile and anoxic stock solutions (per liter): 10 mL of Wolin's vitamin solution (, 1.64 g Na-acetate, 10 g glycerol (for *C. pasteurianum* and co-cultures), and as needed of Na₂-fumarate. All these solutions were sterilized by autoclaving, except for the vitamin solution, which was sterilized by filtration (0.2 µm). Syringes and needles were flushed with N₂ prior to inoculation, addition of solutions, and sampling to prevent the entry of oxygen into the culture bottles. The final pH of the medium was 6.8.

Experimental set-up

Prior to co-cultures and controls, *C. pasteurianum* was first grown with the DSMZ 54b medium and then transferred in M1 medium supplemented with glucose (10 g/L) first, and then subcultured in M1 medium with glycerol (10 g/L) as substrate for 24h. After that, one mL of the pre-culture (1.8×10^7 cells mL⁻¹) was used to inoculate 50 mL of medium during the batch assays. Simultaneously, 1 mL of a concentrated pre-culture of *G. sulfurreducens* (2.1×10^8 cells mL⁻¹) was also used as co-inoculum. The concentrated pre-culture was prepared as follows: 50 mL of *G. sulfurreducens* culture (2.1 days) were centrifuged at 3600 g for 10 minutes and the pellet was re-suspended in two mL of fresh medium. Both strains were co-cultivated under four conditions (with 130 mM glycerol and 20 mM acetate in all cases): 1) Glycerol/Acetate; 2) Glycerol/Acetate + 2.5 mM fumarate; 3) Glycerol/Acetate + 10 mM

fumarate; and 4) Glycerol/Acetate + 40 mM fumarate. 40 mM of fumarate being the typical amount used during culturing of *G. sulfurreducens*, was set as the maximal concentration. *G. sulfurreducens* was cultivated under the four previously conditions mentioned as controls, and *C. pasteurianum* was cultivated only under condition 4 (with 40 mM of fumarate). Inoculated bottles were incubated under continuous mixing at 35°C. All pure culture controls and co-culture batch assays were performed in triplicate.

Growth monitoring

Both optical density (OD) and Quantitative Real-Time polymerase chain reaction (qPCR) were used to monitor the growth of *G. sulfurreducens* and *C. pasteurianum*. The OD was measured using a Helios Epsilon spectrophotometer (Thermo Scientific) at a wavelength of 600 nm. DNA extractions were performed with the FastDNA™ SPIN Kit for Soil (MP Biomedicals™), according to the recommendations of the manufacturer. PCRs were performed as reported before (Moscoviz et al. 2017b) using 96-well real-time PCR plates (Eppendorf, Hamburg, Germany) and Biorad CFX96 system (Biorad, Hercules, USA). The average number of 16S rRNA gene copies per cell obtained for *G. sulfurreducens* and *C. pasteurianum* were divided by a factor of 2 and 10 respectively (Berthomieu et al. 2022) to calculate the average number of cells of each strain.

Growth rate calculations

The optical density (OD_{600nm}) data were fitted with the *Growthcurver* (Sprouffske and Wagner 2016) software package of R based on the logistic equation 1 to calculate the intrinsic growth rates (r) during the exponential phase.

$$N_t = \frac{K}{1 + \left(\frac{K-N_0}{N_0}\right) e^{-rt}} \dots\dots\dots\text{Eq. 1}$$

Where N_t represents the population size at any time t ; N_0 is the population size at the beginning of the growth curve; K is the maximum possible population size in a particular

condition also known as carrying capacity; and r is the intrinsic growth rate under ideal conditions.

Analytical methods

Fumarate, glycerol, acetate, and the other end products were measured by HPLC using an Aminex HPX-87H (Bio-Rad) column with 2.5 mM H₂SO₄ as the mobile phase. Samples were first centrifuged at 12,000 g for 15 min and then supernatants were filtered with 0.2 μ m syringe nylon filters, as described elsewhere (Berthomieu et al. 2022).

Electron balance calculations

The electron equivalents (e_{eq}^-) of each metabolite at the beginning and at the end of the fermentations were calculated as previously reported (Moscoviz et al. 2017b) by multiplying the molar amount of each metabolite by their electron molar equivalents (*i.e.* number of electrons that can be recovered per molecule upon complete oxidation): Glycerol ($e_{eq}^- = 14$), acetate ($e_{eq}^- = 8$), 1,3-PDO ($e_{eq}^- = 16$), ethanol ($e_{eq}^- = 12$), butyrate ($e_{eq}^- = 20$), butanol ($e_{eq}^- = 24$), and lactate ($e_{eq}^- = 12$).

Statistical tests

The statistical analyses of the data were conducted through a one-way analysis of variance (ANOVA) using Microsoft Excel™. Upon detection of significant differences, a post-hoc Tukey's honest significant difference (HSD) test was performed as described by Haynes (2013). The Tukey's test permits a pairwise comparison to identify significant differences between groups. The significance level was set at 5 % (P -value=0.05).

RESULTS

Growth of *G. sulfurreducens* and *C. pasteurianum* in pure culture and co-cultures

Initially, OD_{600nm} measurements were conducted to monitor the growth kinetics (Fig. 1). Notably, the lag phase was substantially shortened in all co-culturing assays. There was a minimal impact on the intrinsic growth rate of *C. pasteurianum*; 0.42 h^{-1} for the pure culture and 0.46 h^{-1} , $0.44 \pm 0.05\text{ h}^{-1}$, $0.41 \pm 0.02\text{ h}^{-1}$, $0.47 \pm 0.11\text{ h}^{-1}$ for the co-cultures with 0 mM, 2.5 mM, 10 mM and 40 mM of fumarate, respectively. The reduction of the lag phase for *C. pasteurianum* during co-culture with *G. sulfurreducens* agrees with previous findings (Berthomieu et al. 2022), confirming the synergetic effect on the co-culture kinetics.

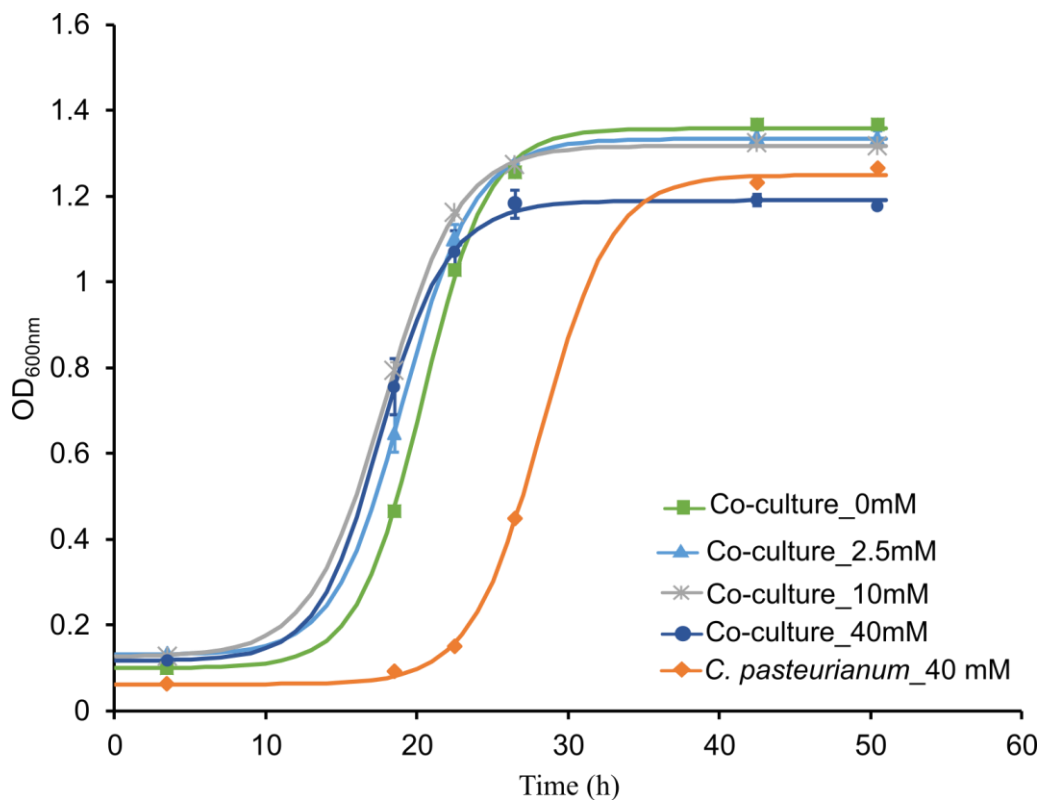


Figure 1. Kinetic growth of *C. pasteurianum* in pure culture with 40 mM of fumarate and co-cultures with 0; 2.5; 10; and 40 mM of fumarate and. *C. pasteurianum* pure culture growth curve corresponds to a single culture, one culture showed no growth while the third grew posteriorly, reaching a similar final optical density. Markers: experimental data; straight lines: fitting model.

Furthermore, qPCR analysis (refer to supplementary Fig. S1) indicated concomitant growth of *C. pasteurianum* and *G. sulfurreducens* in all co-culture conditions. Specifically, in co-culture experiments without fumarate addition, an initial increase in *G. sulfurreducens* cells was followed by a rapid decay phase occurring around 26 hours. This decay phase of *G. sulfurreducens* was notably slower in co-cultures with 2.5 mM and 10 mM of fumarate. Finally, with 40 mM of fumarate, no decay phase was observed, and the co-culture maintained a stationary phase beyond 50 hours.

To evaluate whether the co-culture with *C. pasteurianum* had an impact on *G. sulfurreducens* growth, the maximal cell amounts of *G. sulfurreducens* that were produced in pure culture and in co-culture were compared (Fig. 2).

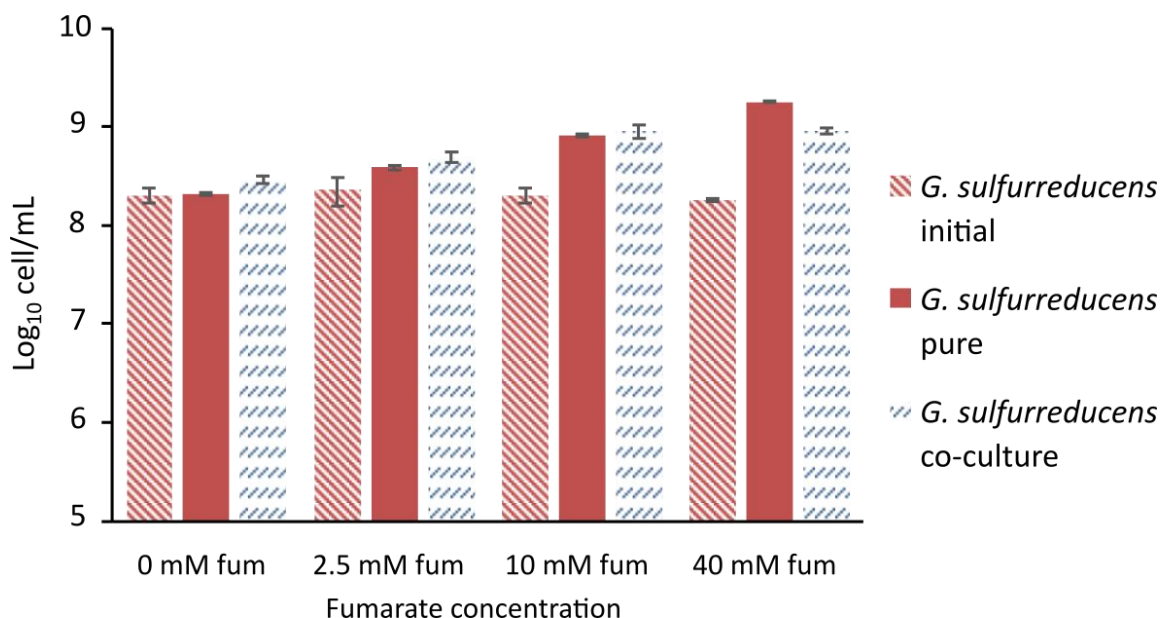


Figure 2. Max qPCR-based counts comparison of *G. sulfurreducens* cells in pure cultures and in co-cultures at different fumarate concentrations. Points were chosen based on the kinetic graphs (Supplementary Fig. S1) and or fumarate consumption. For assays with 0, 2.5, and 10 mM of fumarate the points compared correspond to the samplings at 22.5 hours. For the for assays with 40 mM fumarate the maximum number of cells was observed after 42.5 hours. The initial number of *G. sulfurreducens* cells, correspond to the average number of the pure culture and co-culture at each condition.

In pure cultures without fumarate, no growth was observed ($2.09 \pm 0.08 \times 10^8$ cell mL⁻¹), whereas significant growth of *G. sulfurreducens* occurred in co-cultures ($2.86 \pm 0.25 \times 10^8$ cells mL⁻¹), representing a $37 \pm 3\%$ increase compared to pure cultures (P-value=0.011, see supplementary Tables S1, S2, S3). In pure cultures supplemented with fumarate, the biomass increased proportionally with fumarate concentration but the increase percentage compared with their respective pure controls gradually decreased ($28 \pm 3\%$ and $9.7 \pm 1\%$ with 2.5 mM and 10 mM respectively). The maximal number of cells per mL observed in the cultures with 2.5 mM of fumarate were $3.88 \pm 0.20 \times 10^8$ and $4.99 \pm 0.58 \times 10^8$ in pure and co-cultures respectively. For cultures with 10 mM of fumarate were $8.16 \pm 0.36 \times 10^8$, and $8.95 \pm 1.30 \times 10^8$ cells mL⁻¹ in the pure and co-cultures respectively. In contrast, a drastic reduction of biomass of $-49 \pm 3\%$ was observed in the co-cultures with 40 mM of fumarate, when compared to the biomass obtained in pure cultures ($9.09 \pm 0.55 \times 10^8$ and $1.79 \pm 0.04 \times 10^9$ cells mL⁻¹ respectively).

Concerning *C. pasteurianum*, despite the shortening of the lag phase during co-culturing, the final number of cells was negatively affected in all the conditions (see Supplementary Fig. S2). The biomass decreased by $66 \pm 4\%$, $73 \pm 2\%$, $63 \pm 2\%$ and $37 \pm 3\%$ for the co-cultures in presence of 0, 2.5, 10 and 40 mM of fumarate respectively.

Metabolic shifts on glycerol fermentation patterns of *C. pasteurianum*

The impact of co-culturing *C. pasteurianum* with *G. sulfurreducens* at different fumarate concentrations was not only reflected on the growth kinetics and biomass but also on the final metabolite distributions of the glycerol fermentations (Fig. 3). An almost complete and similar glycerol depletion was achieved under pure and co-culture conditions, with final concentrations of 0.20 ± 0.06 g/L and 0.27 ± 0.08 g/L respectively. The final pH values were also similar for all conditions (5.6 and 5.7 for pure and co-culture conditions respectively).

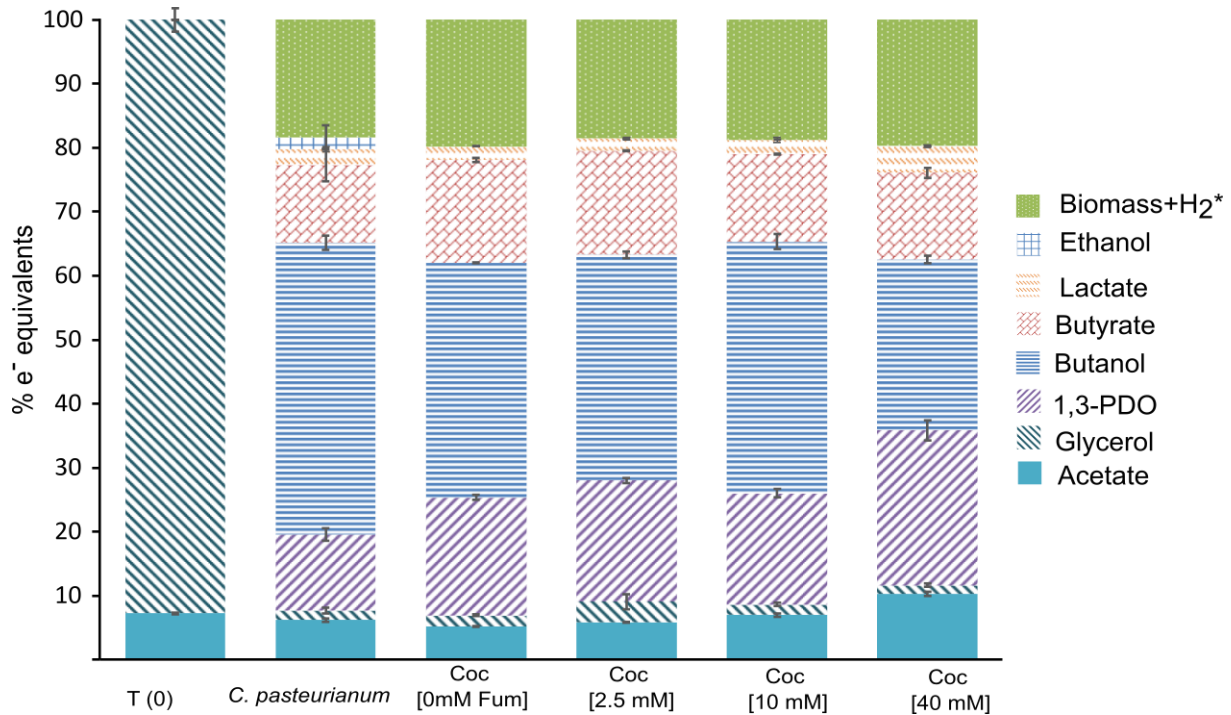


Figure 3. Distributions of electron equivalents in metabolites found at the beginning and at the end of glycerol fermentations by *C. pasteurianum* in pure cultures and co-cultures. Fumarate, succinate, and malate were not considered since they are not related to *C. pasteurianum* metabolism. *Theoretical biomass and H₂ electron equivalents.

The main metabolites produced during glycerol fermentation were butanol, 1,3-PDO, and butyrate, representing together $70 \pm 5\%$, $71 \pm 1\%$, $70 \pm 1\%$, $70 \pm 2\%$, and $64 \pm 3\%$ of the electrons recovered in pure cultures of *C. pasteurianum* and co-cultures with 0, 2.5, 10 and 40 mM of fumarate respectively. Less than 10% of the electrons recovered corresponded to acetate, lactate, and ethanol. In agreement with previous reports (Moscoviz et al. 2017b; Berthomieu et al. 2022), a metabolic shift was observed in all co-culturing conditions, characterized by an increase in 1,3-PDO yield and a concurrent decrease in butanol yield (Table 1).

Table 1. Comparison of butanol and 1,3-PDO yields (**g/g** glycerol) of *C. pasteurianum* in pure and in co-culture with *G. sulfurreducens* under different conditions.

Fumarate Yield (g/g glycerol)/	<i>C. pasteurianum</i>		Co-culture				<i>C. pasteurianum</i>	
	40 mM	0 mM	2.5 mM	10 mM	40 mM	0 mM	0 mM	
	This study				Moscoviz et al. 2017			
Butanol	0.23 ± 0.01	0.19 ± 0.003	0.19 ± 0.004	0.20 ± 0.01	0.14 ± 0.005	0.19 ± 0.01	0.17 ± 0.002	
1,3-PDO	0.09 ± 0.01	0.15 ± 0.004	0.16 ± 0.01	0.14 ± 0.01	0.20 ± 0.02	0.13 ± 0.01	0.16 ± 0.004	

* Co-culture results correspond to the highest 1,3-PDO yield achieved.

Indeed, the butanol yields significantly decreased (P -value = 1.75E-09, see supplementary Table S4, S5, S6) in all co-cultures when compared with the yield achieved in the pure cultures of *C. pasteurianum* (0.23 ± 0.01 g_{butanol}/g_{glycerol}). The maximal yield decrease ($-37 \pm 2\%$) occurred at the highest fumarate concentration (40 mM), achieving 0.14 ± 0.005 g_{butanol}/g_{glycerol}. The butanol yield decreases in the co-culture with 0 mM and 2.5 mM ($-17 \pm 0.1\%$ and $-16 \pm 2\%$ respectively) were not significantly different between them. Lastly, the co-culture with 10 mM fumarate showed the lowest butanol yield decrease ($-11 \pm 3\%$).

Inversely to butanol, 1,3-PDO yields increased in the co-cultures. A significant increase was observed (P -value = 1.65E-07, see supplementary Tables S4, S7, S8), regardless of the co-culture condition, in comparison with the yield observed in the pure culture of *C. pasteurianum* (0.09 ± 0.01 g_{PDO}/g_{glycerol}). As an illustration, 1,3-PDO yields increased by more than 50 % in the co-cultures supplemented with 0, 2.5, and 10 mM of fumarate (61 ± 5 %, 71 ± 7 %, and 51 ± 8 % respectively). The 1,3-PDO yield remarkably increased in the co-cultures at 40 mM of fumarate ($+120 \pm 20\%$), this result being also significantly different from the other co-culture assays.

Additional controls of *C. pasteurianum* were conducted (see Supplementary Figure S3), and the influence of fumarate and acetate addition on the produced succinate during fumarate reduction on the enhanced 1,3-PDO yields during glycerol fermentation in the co-cultures was ruled out. Berthomieu et al. (2022) have already dismissed the potential competition for trace compounds such as Fe (II), cobalt, or chelated cobalt, as a possible

reason behind the observed metabolic shifts in the co-cultures. For the third major metabolite (*i.e.* butyrate), no significant difference (P -value = 0.094) was observed regardless of the studied condition. Regarding the final acetate concentrations related to glycerol fermentations, the theoretical quantities of acetate oxidized by *G. sulfurreducens* in the co-cultures were calculated and summed (Supplementary Table S9.). These theoretical acetate amounts were calculated according to the succinate produced, taking as basis the *G. sulfurreducens* pure controls cultivated with 40 mM of fumarate (0.34 mole acetate consumed per mole of succinate produced). The hypothetical amounts of acetate consumed when using *C. pasteurianum* as electron acceptor were not considered. In the case of the co-cultures without and with 2.5 mM of fumarate, the final acetate concentrations (13.2 ± 0.2 mM and 14.9 ± 0.4 mM respectively) were slightly lower than the *C. pasteurianum* pure cultures (15.8 ± 0.6 mM), without significant difference compared to the pure controls for both cases. Finally, acetate production was promoted for the co-cultures with 10 mM and 40 mM of fumarate, especially for the latter (17.8 ± 0.9 mM and 26.2 ± 1.2 mM respectively). Both cases were significantly different in regard to the pure cultures (see Supplementary Table S10, S11).

Lastly, the final biomass and H₂ concentrations in pure and in co-culture of *C. pasteurianum*, were estimated based on the electron balances of the measured metabolites. Interestingly, differing from qPCR analyses (Supplementary Fig. S2), the biomass+H₂ production seemed poorly affected by the co-culture. The quantified products represented around 80% of electron equivalent whatever the studied condition.

Fumarate reduction by *G. sulfurreducens* in co-culture and pure culture

The metabolite dynamics associated with *G. sulfurreducens* metabolism in both pure cultures and co-cultures supplemented with 40 mM of fumarate are illustrated in Fig. 4. In pure cultures (Fig. 4A), fumarate reduction followed a classic pattern, characterized by a concomitant acetate oxidation and the complete conversion of fumarate (37.2 ± 0.2 mM) to succinate (37.2 ± 0.7 mM). A transient accumulation of malate was also observed,

consistent with previous findings during *G. sulfurreducens* pure cultures with acetate and fumarate (Galushko and Schink 2000; Geelhoed, Henstra and Stams 2016). Transient malate accumulation occurs due to its thermodynamically unfavorable oxidation to oxaloacetate coupled with NAD⁺ reduction ($\Delta G^{\circ} \approx +30$ kJ per mole malate at pH 7). To deal with this, *G. sulfurreducens* accumulates malate and maintains low oxaloacetate levels through efficient removal via the citrate synthase reaction (Galushko and Schink 2000). In contrast, in co-culture conditions (Fig. 4B), fumarate reduction kinetics were different, with a notable decrease in the rate of fumarate consumption by approximately 54.8%. While fumarate was completely depleted in pure cultures after approximately 42 hours, 7 mM of fumarate persisted in the case of the co-cultures.

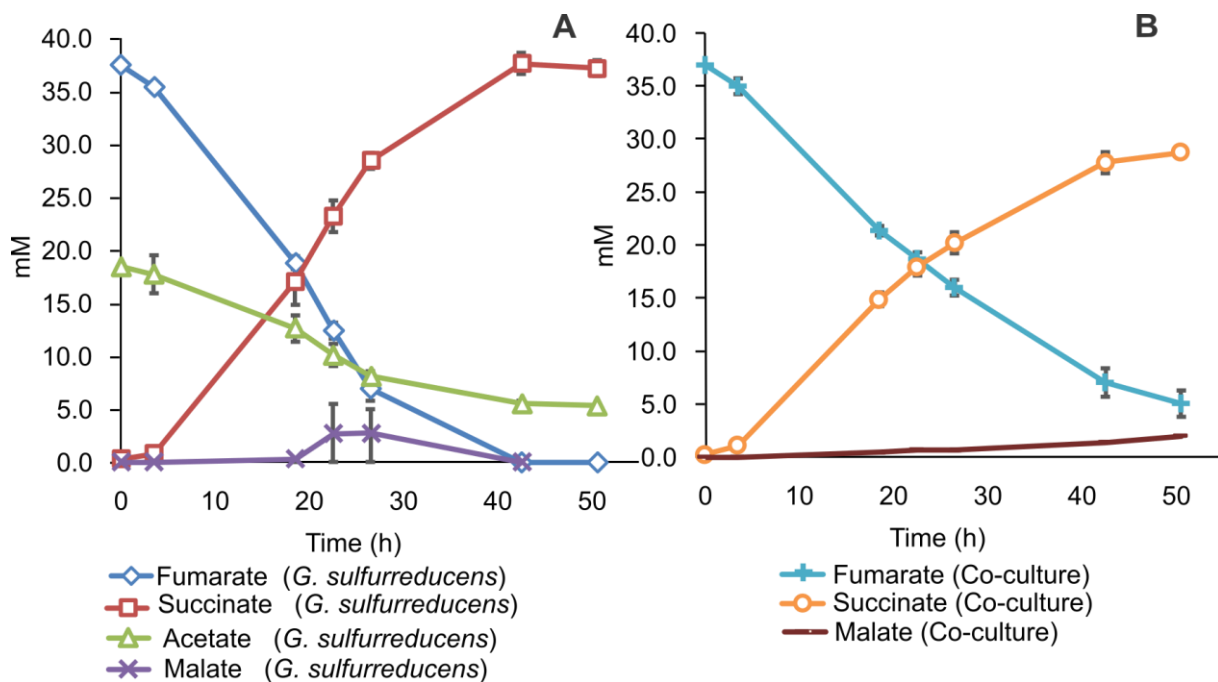


Figure 4. Fumarate consumption and succinate production profiles by *G. sulfurreducens* during pure (A) and co-culture (B) experiments with 40 mM of fumarate. Acetate concentration in the co-culture (B) is not shown because it is simultaneously consumed by *G. sulfurreducens* and produced by *C. pasteurianum*.

A final sampling after 100 hours, showed that 0.5 mM of fumarate remained unconsumed in the co-cultures, while the final molar succinate concentrations were not equivalent to the fumarate consumed (31.7 ± 1.8 mM and 37.2 ± 0.2 mM, respectively).

Additionally, a small but irreversible formation of malate (2.7 mM) and trace amounts of formate (between 2.5 and 3.2 mM) were detected in the co-cultures supplemented with 40 mM of fumarate. Overall, the sum of the final molar concentrations of malate, succinate, and fumarate in the co-cultures (34.5 ± 1.8 mM) was slightly lower on average than the initial fumarate concentration (37.2 ± 0.2 mM). This suggests that a small amount of the fumarate (approximately 2.7 mM) was used as a carbon source, which aligns with the detected amounts of formate.

DISCUSSION

The reduction of the lag phase observed in the co-cultures of *G. sulfurreducens* and *C. pasteurianum*, regardless of the conditions, appears to be a common feature. Similar observations were reported in a study dealing with a denitrifying microbial community bio-augmented with *G. sulfurreducens*. In this study, the usual 15-hour lag phase observed in the non-augmented community was significantly reduced, leading to an improvement in denitrification rates (Wan *et al.* 2018). One hypothesis to explain how *G. sulfurreducens* could enhance the initial growth of its partner during IET, suggests that external cytochromes may act as 'iron lungs' or 'bio-capacitors,' capable of storing electrons that can be readily transferred when an electron acceptor is available (Lovley 2008; Esteve-Núñez *et al.* 2011; Estevez-Canales *et al.* 2015). Another explication involves the release of molecules such as cobamides or a heme derivatives as proposed by Berthomieu *et al.* (2022), which could improve cellular activity. Recently, Zhang *et al.* (2023) observed the same lag phase reduction effect in co-cultures of *G. sulfurreducens* and *C. pasteurianum* along with a boost on hydrogen production during glucose fermentation. They reported a buffer effect when adding *G. sulfurreducens*, which increased in turn the amounts of glucose consumed. Still, the exact mechanism explaining how the microorganisms interact to instantly favor the growth of *C. pasteurianum* by shortening the lag phase remains to be fully elucidated.

On the other hand, the diminution in biomass yields of *C. pasteurianum* during co-culture, as shown by the qPCR analysis, are in concordance with prior observations (Moscoviz *et al.* 2017b). Similarly, estimations of H₂+biomass (~19% electron equivalents) based on electron balances of the measured metabolites, agree with the results reported by Moscoviz *et al.* (2017b). However, our findings seem to underestimated H₂+biomass for the pure cultures, contrasting with their study, where it accounted for approximately 24% of electrons equivalents. Such discrepancies may be attributed to high deviations for the butyrate concentrations observed in the pure cultures. Decreases on biomass yield ranging from 14 to 41% has been previously reported in fermentative species when provided with extracellular electron supply (Moscoviz *et al.* 2017a, 2020). According to Moscoviz *et al.* (2017a), several factors may contribute to such biomass diminutions, their thermodynamic analysis suggests that, especially in the case of IET, it might be due to non-mutualistic interactions. Interestingly, the growth of *C. pasteurianum* appeared to be less affected at higher fumarate concentrations, indicating a potential less intensive IET with *G. sulfurreducens*. However, a more pronounced metabolic shift towards increased 1,3-PDO production was observed at the highest fumarate concentration. This confirms the observations made by Berthomieu *et al.* (2022), suggesting that IET is not the main responsible of the metabolic shift, but instead a molecule produced during *G. sulfurreducens* growth plays a major role.

The increased growth of *G. sulfurreducens*, in co-cultures with 0 mM and 2.5 mM fumarate, compared to the pure culture controls, suggests that *C. pasteurianum* was utilized as a terminal electron acceptor (TEA) by *G. sulfurreducens* under those conditions. Conversely, in co-cultures with higher fumarate concentrations, the lower biomass of *G. sulfurreducens* compared to their respective pure culture controls indicates the utilization of an external electron acceptor rather than fumarate. A decrease in *G. sulfurreducens* biomass (-72% biomass yield) was previously reported when using an external TEA [Fe (III)] instead of fumarate (Esteve-Núñez, Núñez and Lovley 2004; Esteve-Núñez *et al.* 2005). This decrease during EET processes can be attributed to the energetically expensive proton

translocation required, while proton production occurs inside the cell, electrons are transferred outside. This unique phenomenon, where the proton gradient negatively affects ATP production, is observed during the reduction of electron acceptors outside the cell, such as Fe (III) and S° (Esteve-Núñez *et al.* 2005). Further explanation for this phenomenon is provided by Mahadevan *et al.* (2006), whose constraint-based model resulted in a theoretical maximum yield of only 0.5 mole of ATP/mole of acetate with Fe (III) as the electron acceptor, compared to 1.5 mole of ATP/mole of acetate during fumarate reduction.

The fumarate reduction patterns observed in the co-cultures supplemented with 40 mM of fumarate, provided further evidence of IET. As mentioned above, small amounts of malate and formate accumulation were observed. Malate accumulation has been previously reported in assays with fumarate in excess (Frühauf-Wyllie and Holtmann, 2022), where transitory concentrations from 5 mM to up to 17 mM were reached with acetate/fumarate ratios of 1:2.5 and 1:5 respectively. This phenomenon occurs due to limited acetate concentration, resulting in insufficient acetyl coenzyme A (CoA) for directing oxaloacetate towards the citrate synthase reaction during the open TCA cycle. However, in our study, acetate was not limiting. Therefore, malate accumulation could be associated with another phenomenon observed by Esteve-Núñez *et al.* (2004), who reported an irreversible malate (≈ 14.2 mM) and formate (≈ 13.8 mM) accumulation when fumarate and Fe (III) were simultaneously added as TEA for *G. sulfurreducens* growing on acetate. In this case, *G. sulfurreducens* exhibited a preferential use of Fe (III) over fumarate. The addition of Fe (III) resulted in a drastic reduction of mRNA levels for the fumarate reductase operon *frdCAB*. Consequently, fumarate was used as an electron donor and converted to Acetyl-CoA via malate and pyruvate, with the formation of formate. Once all Fe (III) was spent, fumarate reduction resumed. In contrast to this, in our study fumarate reduction was not completely inhibited but it appeared to co-occur. This can be explained simply because, unlike Fe (III), which is readily available for reduction, the electron transfer to *C. pasteurianum* is more complex, depending on its growth and is likely not a priority when a fermentable substrate is available. The lower amounts of malate and formate detected may also indicate a more

restricted use of fumarate as electron donor. The preference for an external TEA over fumarate was not expected, as the latter is a more reliable source to support growth (Esteve-Núñez *et al.* 2005). However, it appears that the use of fumarate as carbon source is more beneficial when other TEAs are available. As suggested by Esteve-Núñez, Núñez and Lovley (2004), this may be a strategy acquired by *Geobacter* species in anoxic subsurface environments where Fe (III) is abundant, and carbon sources are scarce.

Our observations along with the literature revised are resumed in Fig. 5, and in conclusion, the growth of *G. sulfurreducens* observed in the co-cultures with *C. pasteurianum* in absence of fumarate, as well as the use of fumarate as electron donor instead of electron acceptor at high fumarate concentrations, provides strong evidence of interspecies electron transfer between these two strains. Notably, the simultaneous growth of both partners and the drastic reduction in the lag phase of *C. pasteurianum* suggest enhanced cellular activity in the co-culture.

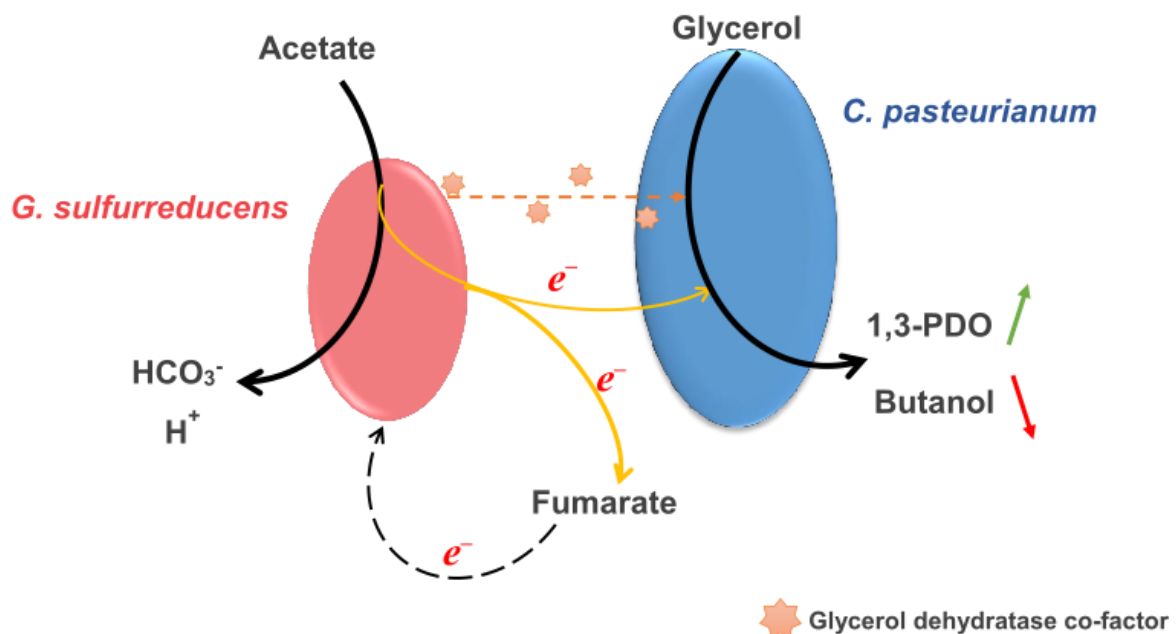


Figure 5. Scheme illustrating the hypothetical interactions between *C. pasteurianum* and *G. sulfurreducens* in co-cultures. Glycerol fermentation by *C. pasteurianum* shifts towards a higher 1,3-PDO yield as a consequence of interspecies electron transfer (IET) and the exchange of cobamide-like molecules, which are excreted by *G. sulfurreducens*. Additionally, fumarate is partially utilized as an electron donor instead of an electron acceptor by the latter.

Initially, it was hypothesized that the presence of a soluble electron acceptor such as fumarate might negatively impact the interaction between these strains or the metabolic shifts. However, our observations revealed a metabolic shift in all co-culture conditions, with higher fumarate leading to an amplified metabolic shift. This increased metabolic shift at higher fumarate concentrations could be attributed higher amounts of cobamides-like molecules produced by *G. sulfurreducens*, which, as reported previously, may drive *C. pasteurianum* towards increased 1,3-PDO production from glycerol. These findings highlight the potential of co-cultures involving EABs like *G. sulfurreducens* and fermenters as a promising strategy to enhance the 1,3-PDO production from glycerol. Moreover, they open the possibility to explore other EABs-fermenters couples as an alternative electrode-fermenters approach applied to electro-fermentation processes.

Acknowledgments

María Fernanda Pérez-Bernal thanks the Consejo Nacional de Ciencia y Tecnología (CONACyT, Mexico) for the grant assigned (no. 711209) for the post-doctoral stay. Special thanks to Gaëlle Santa-Catalina for the qPCR analyses performed.

Conflict of interest: The authors declare that they have no known competing financial interests or personal relationships that could have appeared to influence the work reported in this paper.

Funding

María Fernanda Pérez Bernal was funded by the Consejo Nacional de Ciencia y Tecnología (CONACyT, Mexico) with a postdoctoral grant.

Availability of data and material

All relevant data are included in the article and/or its supplementary information files. Detailed information is available upon reasonable request.

Authors' Contributions:

María Fernanda Pérez Bernal (conceptualization, formal analysis, funding acquisition, investigation, writing – original draft, writing – review and editing), Roland Berthomieu (writing – original draft, writing – review and editing), Elie Desmond-Le Quéméner (formal analysis, supervision, writing – review and editing), Nicolas Bernet (supervision, writing – review and editing, resources), Eric Trably (conceptualization, supervision, writing – review and editing).

REFERENCES

- Benomar S, Ranava D, Cárdenas ML *et al.* Nutritional stress induces exchange of cell material and energetic coupling between bacterial species. *Nat Commun* 2015;6:6283
- Berthomieu R, Pérez-Bernal MF, Santa-Catalina G *et al.* Mechanisms underlying *Clostridium pasteurianum*'s metabolic shift when grown with *Geobacter sulfurreducens*. *Appl Microbiol Biotechnol* 2022;106:865–76.
- Choi O, Sang BI. Extracellular electron transfer from cathode to microbes: Application for biofuel production. *Biotechnol Biofuels* 2016;9:1–14.
- Esteve-Núñez A, Busalmen JP, Berná A *et al.* Opportunities behind the unusual ability of *geobacter sulfurreducens* for exocellular respiration and electricity production. *Energy Environ Sci* 2011;4:2066–9.
- Esteve-Núñez A, Núñez C, Lovley DR. Preferential Reduction of Fe(III) over Fumarate by *Geobacter sulfurreducens*. *J Bacteriol* 2004;186:2897–9.
- Esteve-Núñez A, Rothermich M, Sharma M *et al.* Growth of *Geobacter sulfurreducens* under nutrient-limiting conditions in continuous culture. *Environ Microbiol* 2005;7:641–8.
- Estevez-Canales M, Kuzume A, Borjas Z *et al.* A severe reduction in the cytochrome C content of *Geobacter sulfurreducens* eliminates its capacity for extracellular electron transfer. *Environ Microbiol Rep* 2015;7:219–26.
- Frühauf-Wyllie HM, Holtmann D. *Geobacter sulfurreducens* metabolism at different donor/acceptor ratios. *MicrobiologyOpen* 2022;11:e1322.
- Galushko AS, Schink B. Oxidation of acetate through reactions of the citric acid cycle by *Geobacter sulfurreducens* in pure culture and in syntrophic coculture. *Arch Microbiol* 2000;174:314–21.
- Geelhoed JS, Henstra AM, Stams AJMM. Carboxydrotrophic growth of *Geobacter sulfurreducens*. *Appl Microbiol Biotechnol* 2016;100:997–1007.
- Haynes W. Tukey's Test. *Encyclopedia of Systems Biology*. Springer, New York, NY, 2013, 2303–4.
- Hungate RE. Chapter IV A Roll Tube Method for Cultivation of Strict Anaerobes. *Methods in Microbiology*. Vol 3. Academic Press, 1969, 117–32.
- Kato S. Biotechnological Aspects of Microbial Extracellular Electron Transfer. *Microbes Environ* 2015;30:133–9.
- Kracke F, Lai B, Yu S *et al.* Balancing cellular redox metabolism in microbial electrosynthesis and electro fermentation – A chance for metabolic engineering. *Metab Eng* 2018;45:109–20.
- Kracke F, Vassilev I, Krömer JO. Microbial electron transport and energy conservation - The foundation for optimizing bioelectrochemical systems. *Front Microbiol* 2015;6:1–18.

- Krasňan V, Plž M, Marr AC *et al.* Intensified crude glycerol conversion to butanol by immobilized *Clostridium pasteurianum*. *Biochem Eng J* 2018;134:114–9.
- Lovley DR. Extracellular electron transfer: Wires, capacitors, iron lungs, and more. *Geobiology* 2008;6:225–31.
- Lovley DR, Ueki T, Zhang T *et al.* Geobacter: The microbe electric's physiology, ecology, and practical applications. *Adv Microb Physiol* 2011;59:1–100.
- Mahadevan R, Bond DR, Butler JE *et al.* Characterization of metabolism in the Fe(III)-reducing organism *Geobacter sulfurreducens* by constraint-based modeling. *Appl Environ Microbiol* 2006;72:1558–68.
- Miller TL, Wolin MJ. A Serum Bottle Modification of the Hungate Technique for Cultivating Obligate Anaerobes. *Appl Microbiol* 1974;27:985–7.
- Moon C, Hwan Lee C, Sang B-II *et al.* Optimization of medium compositions favoring butanol and 1,3-propanediol production from glycerol by *Clostridium pasteurianum*. *Bioresour Technol* 2011;102:10561–8.
- Moscoviz R, Desmond-Le Quéméner E, Trably E *et al.* Novel Outlook in Microbial Ecology: Nonmutualistic Interspecies Electron Transfer. *Trends Microbiol* 2020;28:245–53.
- Moscoviz R, Flayac C, Desmond-Le Quéméner E *et al.* Revealing extracellular electron transfer mediated parasitism: energetic considerations. *Sci Rep* 2017a;7:1–9.
- Moscoviz R, de Fouchécour F, Santa-Catalina G *et al.* Cooperative growth of *Geobacter sulfurreducens* and *Clostridium pasteurianum* with subsequent metabolic shift in glycerol fermentation. *Sci Rep* 2017b;7:44334.
- Moscoviz R, Toledo-Alarcón J, Trably E *et al.* Electro-Fermentation: How To Drive Fermentation Using Electrochemical Systems. *Trends Biotechnol* 2016;34:856–65.
- Potter MC. Electrical Effects Accompanying the Decomposition of Organic Compounds. *Proc R Soc B Biol Sci* 1911;84:260–76.
- Sprouffske K, Wagner A. Growthcurver: An R package for obtaining interpretable metrics from microbial growth curves. *BMC Bioinformatics* 2016;17:1–4.
- Wan Y, Zhou L, Wang S *et al.* Syntrophic Growth of *Geobacter sulfurreducens* Accelerates Anaerobic Denitrification. *Front Microbiol* 2018;9:1–8.
- Zhang Y, Zheng S, Hao Q *et al.* Respiratory electrogen *Geobacter* boosts hydrogen production efficiency of fermentative electrotoph *Clostridium pasteurianum*. *Chem Eng J* 2023;456:141069.